SCIENCE CHINA
Technological Sciences

•Article•

https://doi.org/10.1007/s11431-024-2727-9

Bridging the Fabry–Perot cavity and asymmetric Berreman mode for long-wave infrared nonreciprocal thermal emitters

CHEN ZiHe[1], YU ShiLv[1] & HU Run[1,2,3*]

[1]*School of Energy and Power Engineering, Huazhong University of Science and Technology, Wuhan 430074, China;*
[2]*Wuhan National Laboratory for Optoelectronics, Huazhong University of Science and Technology, Wuhan 430074, China;*
[3]*Department of Applied Physics, Kyung Hee University, Gyeonggi-do 17104, Republic of Korea*

Received January 30, 2024; accepted June 26, 2024; published online September 14, 2024

The long-wave infrared band (8–14 μm) is essential for several applications, such as infrared detection, radiative cooling, and near-field heat transfer. However, according to Kirchhoff's law, the intrinsic balance between thermal absorption and emission limits the further improvement of photon energy conversion and thermal management. Thus, breaking Kirchhoff's balance and achieving nonreciprocal thermal radiation in the long-wave infrared band are necessary. Most existing designs for nonreciprocal thermal emitters rely on grating or photonic crystal structures to achieve nonreciprocal thermal radiation at narrow peaks, which are relatively complex and typically realize bands larger than 14 μm. Here, a sandwich structure consisting of an epsilon-near-zero (ENZ) magneto-optical layer (MOL), a dielectric layer (DL), and a metal layer is proposed to achieve a strong nonreciprocal effect in the long-wave infrared band, which is mainly attributed to the strengthening of the asymmetric Berreman mode by the Fabry–Perot cavity. In addition, the impact of the incident angle, DL thickness, and DL refractive index on the nonreciprocal thermal radiation has been investigated. Moreover, by replacing the ENZ MOL with the gradient ENZ MOL, the existence of the DL can further improve the nonreciprocity of the broadband nonreciprocal thermal radiation. The proposed work promotes the development and application of nonreciprocal energy devices.

long-wave infrared band, nonreciprocal thermal radiation, sandwich structure, Fabry–Perot cavity, asymmetric berreman mode

Citation: Chen Z H, Yu S L, Hu R. Bridging the Fabry–Perot cavity and asymmetric Berreman mode for long-wave infrared nonreciprocal thermal emitters. Sci China Tech Sci, 2024, 67, https://doi.org/10.1007/s11431-024-2727-9

1 Introduction

The long-wave infrared band (8–14 μm) is the operational band of most infrared detectors or emitters, which is of great significance in understanding the infrared radiation characteristics of objects [1–4]. Traditional designs of infrared detectors or emitters are based on Kirchhoff's radiation law [5–7], which defines the relationship between emission and absorption; that is, emissivity is equal to absorptivity for a given wavelength and angle. In other words, when an object absorbs radiation, part of the energy is returned to the emitter, leading to an inherent energy loss. Therefore, if the emission and absorption processes can be controlled separately in the long-wave infrared band, then new design routes for infrared camouflage [8], radiation cooling [9,10], near-field heat transfer [11–13], and other applications [14–16] can be realized.

Kirchhoff's radiation law is a consequence of the Lorentz reciprocity theorem rather than the second law of thermodynamics, indicating that it is possible to break Kirchhoff's law for nonreciprocal materials, such as magneto-optical (MO) materials, to disobey this detailed equilibrium. In 2014, the groundbreaking work of Zhu and Fan [17] demonstrated that Kirchhoff's law can be violated by breaking

*Corresponding author (email: hurun@hust.edu.cn)

time-reversal symmetry. Since then, nonreciprocal absorption and emission have been predicted in systems designed based on MO materials [17–25], Kerr nonlinearity [26], and time modulation [27]. Among them, MO materials have attracted considerable attention because of their good nonreciprocal characteristics in the infrared band [17,18,28]. Existing designs based on MO materials include grating structures [17,19,21,24] and multilayer photonic crystal structures [22,29], which rely on guided or cavity mode resonances to realize narrowband nonreciprocal thermal radiation at resonant wavelengths. However, broadband emission or absorption is necessary for energy utilization, such as radiative cooling. In response to this requirement, several scholars have proposed a gradient epsilon-near-zero (ENZ) multilayer structure to realize broadband nonreciprocal thermal radiation at ENZ wavelengths via excitation of the Berreman mode [30], which has been experimentally verified [31]. However, the existing utilization of a monolayer ENZ film typically requires placing it on a substrate with a negative dielectric constant to achieve strong nonreciprocal effects [30], which limits its application in practice. In addition, nonreciprocal effects achieved by most of the aforementioned works are usually at wavelengths greater than 14 μm, which cannot meet the needs of the long-wave infrared band. Recently, several designs based on Weyl semimetals can achieve the prediction of nonreciprocal absorption and emission in the long-wave infrared band [32]. However, the strong MO effect of Weyl semimetals has been theoretically realized only at low temperatures and has not been experimentally verified in energy devices at room temperature [33]. Therefore, simpler nonreciprocal narrowband or broadband thermal emitters/absorbers that can satisfy the long-wave infrared band need to be designed and developed.

Here, a sandwich structure consisting of a bottom metal layer (ML), a top ENZ magneto-optical layer (MOL), and a middle dielectric layer (DL), which can achieve a strong nonreciprocal response in the long-wave infrared band, is proposed. The effective impedance theory has been used to explain the nonreciprocity mechanism, which is mainly attributed to the synergistic action of the Fabry–Perot cavity and the Berreman mode. In addition, the effect of the Fabry–Perot cavity on gradient ENZ MO materials is explored, where the nonreciprocal strength of broadband thermal radiation can be enhanced by the presence of Fabry–Perot cavities. This work can further promote the development and utilization of devices for energy conversion and thermal management.

2 Calculation methods

As shown in Figure 1(a), the nonreciprocal emitter consists of a three-layer structure, including a bottom ML (Al), a top ENZ MOL (InSb), and an intermediate DL (Ge). The magnetic field B is along the y-axis, and B = 3 T. Under the

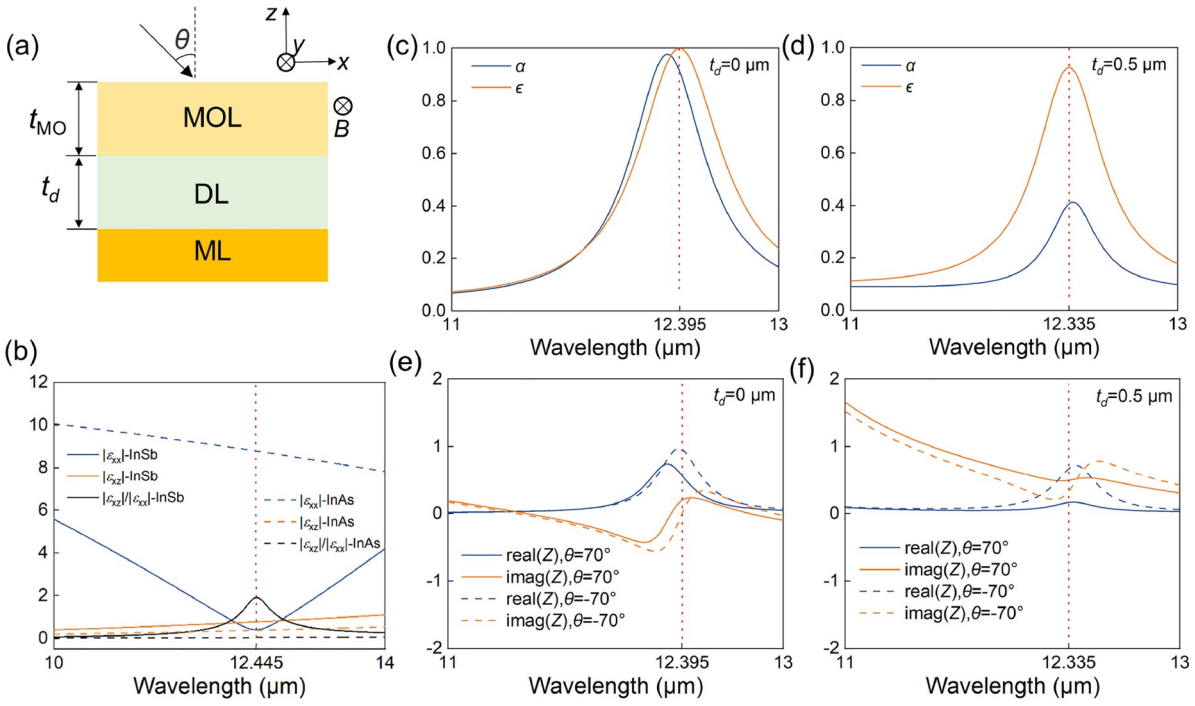

Figure 1 (a) Diagram of a nonreciprocal thermal emitter shaped like a sandwich structure. (b) Material permittivity of the MOL varying with wavelength, and absorptivity and emissivity spectra of the emitter: without the DL (c) and with the DL (d). Effective impedance of the structure: without the DL (e) and with the DL (f).

applied magnetic field, the dielectric tensor of the MO material InSb is asymmetric, that is [30]

$$\varepsilon = \begin{bmatrix} \varepsilon_{xx} & 0 & \varepsilon_{xz} \\ 0 & \varepsilon_{yy} & 0 \\ \varepsilon_{zx} & 0 & \varepsilon_{zz} \end{bmatrix}, \tag{1}$$

where

$$\varepsilon_{xx} = \varepsilon_{zz} = \varepsilon_{\infty} - \frac{\omega_p^2(\omega + \mathrm{i}\Gamma)}{\omega[(\omega + \mathrm{i}\Gamma)^2 - \omega_c^2]}, \tag{2}$$

$$\varepsilon_{xz} = -\varepsilon_{zx} = -\mathrm{i}\frac{\omega_p^2\omega_c}{\omega[(\omega + \mathrm{i}\Gamma)^2 - \omega_c^2]}, \tag{3}$$

$$\varepsilon_{yy} = \varepsilon_{\infty} - \frac{\omega_p^2}{\omega(\omega + \mathrm{i}\Gamma)}. \tag{4}$$

In Eqs. (2)–(4), ε_{∞} is the high-frequency permittivity, and ε_{∞} = 15.68; ω_p is the plasma frequency, and $\omega_p = \sqrt{ne^2/(m^*\varepsilon_0)}$; ω_c is the cyclotron frequency, and $\omega_c = eB/m^*$; Γ is the relaxation rate, and $\Gamma = e/(m^*\mu_n)$. Here, e is the elementary charge, and ε_0 is the vacuum permittivity. n is the doping concentration, and $n = 8\times10^{24}$ m^{-3}. μ_n is the electron mobility, and μ_n = 6400 cm^2 V^{-1} s^{-1} [34]. m^* is the effective electron mass, and $m^* = m_n[1 + \frac{1}{2}(\frac{3}{\pi})^{\frac{2}{3}}(\frac{h^2}{E_g m_n})n^{\frac{2}{3}}]^{\frac{1}{2}}$, where h is Planck's constant, E_g = 0.17 eV is the bandgap energy at 300 K, $m_n = 0.014m_e$ is the electron effective mass at the bottom of the conduction band, and m_e is the resting mass of the electron [30,35]. In addition, germanium (Ge) is chosen as the DL and the refractive index of the DL n_d is 4. The permittivity of the ML (Al) is obtained using the Drude model, which is expressed as follows [19]:

$$\varepsilon_{Al} = \varepsilon_{\infty} - \frac{\omega_p^2}{\omega(\omega + \mathrm{i}\Gamma)}, \tag{5}$$

where ε_{∞}=1, ω_p=2.24×10^{16} rad s^{-1}, and Γ=1.24×10^{14} rad s^{-1}.

The incident wave is a transverse magnetic wave in the x–z plane, and the incident angle θ is 70°. Here, the directional spectral absorptivity α and emissivity ϵ are expressed as follows [17,19]:

$$\alpha(\theta, \lambda) = 1 - R(\theta, \lambda) - T(\theta, \lambda), \tag{6}$$

$$\epsilon(\theta, \lambda) = 1 - R(-\theta, \lambda) - T(-\theta, \lambda), \tag{7}$$

where $R(\theta, \lambda)$ and $T(\theta, \lambda)$ are the directional spectral reflectance and transmittance, respectively. The directional spectral reflectance and transmittance are calculated using the transfer matrix, and the details are provided in Ref. [29].

3 Results and discussion

Under the applied magnetic field, the asymmetric dielectric tensor of MO materials can cause asymmetric angular reflection and absorption to achieve nonreciprocal thermal radiation. The ratio γ of the asymmetric term $|\varepsilon_{xz}|$ to the symmetric term $|\varepsilon_{xx}|$ largely determines the degree of nonreciprocity. Figure 1(b) shows the dielectric properties of the MO materials InAs and InSb in the wavelength range of 10–14 μm, where the dielectric properties of InAs are obtained from Ref. [17]. The value of γ of InAs is only approximately 0.04, whereas the value of γ of InSb reaches 1.91 when the wavelength is 12.445 μm (that is, the ENZ wavelength), which is the reason why InSb is chosen as the MOL. Here, to better excite the Berreman mode of ENZ MO material, according to the generalized Fresnel formula, the thickness t_{MO} of single-layer ENZ film with the minimum reflectivity is calculated using the following equation [36]:

$$t_{MO} = \frac{\lambda_{ENZ}}{2\pi}\frac{\cos\theta}{\sin^2\theta}\left(\mathrm{Im}\left\{\frac{-1}{\varepsilon_{xx}}\right\}\right)_{\max}^{-1}, \tag{8}$$

where θ is the incident angle, ε_{xx} is the symmetric term of the dielectric tensor of the ENZ MO material, and λ_{ENZ} is the ENZ wavelength. According to Eq. (8), t_{MO} = 0.31 μm. In addition, the dielectric material thickness t_d is 0.5 μm, and the ML thickness is 0.2 μm.

3.1 Influence of the DL on the single ENZ MOL

Here, to better compare the impact of the DL on nonreciprocal thermal radiation, the absorption and emission spectra without and with the DL are calculated, as shown in Figure 1(c) and (d), respectively. First, without the DL, the ENZ film is placed directly on the metallic aluminum layer. The absorption and emission spectra are shown in Figure 1(c), and the emissivity is close to 1 at the wavelength of 12.395 μm, indicating that the Berreman mode is well excited near the ENZ wavelength. Second, the absorption and emission curves do not overlap mainly because the asymmetric Berreman mode is excited under the action of the magnetic field, which leads to the nonreciprocity phenomenon near the ENZ wavelength [31]. In addition, the absorption and emission spectra of our proposed sandwich structure are calculated, as shown in Figure 1(d). Strong emission can still be observed near the ENZ wavelength, indicating the excitation of the Berreman mode. The separation degree of the absorption and emission spectra is more obvious, which means that the degree of nonreciprocity has been significantly improved. At the wavelength of 12.335 μm, the emissivity is 0.925, whereas the absorptivity is only 0.407, indicating the enhancement of the asymmetric Berreman mode by the Fabry–Perot cavity. To better explain the internal mechanism, the effective impedance matching theory is used to explain the nonreciprocity phenomenon, which is expressed as follows [37]:

$$Z = \sqrt{\frac{(1+S_{11})^2 - S_{21}^2}{(1-S_{11})^2 - S_{21}^2}}, \tag{9}$$

where S_{11} and S_{21} are the scattering parameters associated with the reflection and transmission coefficients, respectively. According to Eq. (9), the effective impedances of the two structures have been calculated, as shown in Figure 1(e) and (f). As the cause of nonreciprocity is generic, the comparison between the effective impedance of the sandwich structure and the free space impedance Z_0 ($Z_0 = 1$) is taken as an example to explain the nonreciprocal phenomenon. As shown in Figure 1(f), the effective impedances at the opposite incident angles are not equal, which means that the structure has different dispersion relationships at opposite angles. When the incident angle is 70°, the effective impedance $Z = 0.163 + 0.495$i at the wavelength of 12.335 μm is poorly matched with the free space impedance Z_0, indicating weak absorption and strong reflection. By contrast, when the incident angle is −70°, the effective impedance of the structure is $0.671 + 0.331$i, which is a better match with the free space impedance, indicating stronger absorption and weaker reflection at this time. According to Eqs. (6) and (7), when the incident angle is 70°, the spectra exhibit strong emission and weak absorption.

3.2 Influence of the incident angle

Then, the effect of the incident angle on nonreciprocal thermal radiation is investigated. Figure 2(a) and (b) show the variations of the absorption and emission spectra with the incident angle in the absence of the DL, respectively. High absorption and high emission near the ENZ wavelength are present at a large angle, indicating the excitation of Berreman mode. In addition, when the incident angle is lower than 50°, absorption and emission decrease significantly, which indicates that the structure has a certain directional radiation capability. Here, to better reflect the degree of nonreciprocity, the difference between emissivity and absorptivity is calculated, as shown in Figure 2(c). Notably, a weak nonreciprocity phenomenon occurs near the ENZ wavelength under the action of the asymmetric Berreman mode. Figure 2(d) and (e) reflect the relationship between the absorption and emission spectra of the sandwich structure with the incident angle. The spectral distribution is still mainly concentrated around the ENZ wavelength, and the difference between absorption and emission spectra indicates high emission and low absorption at a large angle. The degree of nonreciprocity is also calculated, as shown in Figure 2(f). When the incident angle is between 20° and 80°, a strong nonreciprocal effect is observed. The comparison of the results in Figure 2(c) and (f) reflects the strengthening effect of the Fabry–Perot cavity on the asymmetric Berreman mode.

3.3 Influence of the DL thickness

The effect of the DL thickness on nonreciprocal thermal radiation is also investigated. Figure 3(a) shows the effect of the thickness t_d on the absorption/emission spectrum in the

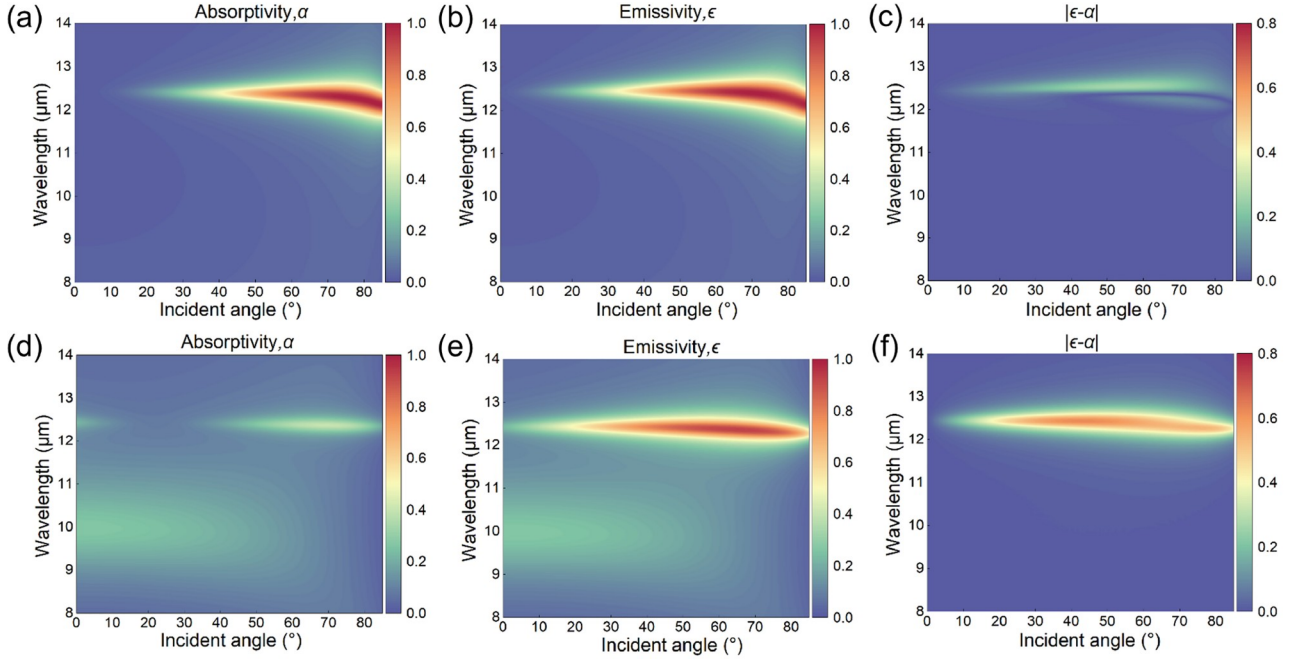

Figure 2 (Color online) Simulated spectra varying with the angle and wavelength of different structures with $B = 3$ T. Absorptivity spectra: without the DL (a) and with the DL (d). Emissivity spectra: without the DL (b) and with the DL (e). Difference between absorptivity and emissivity: without the DL (c) and with the DL (f).

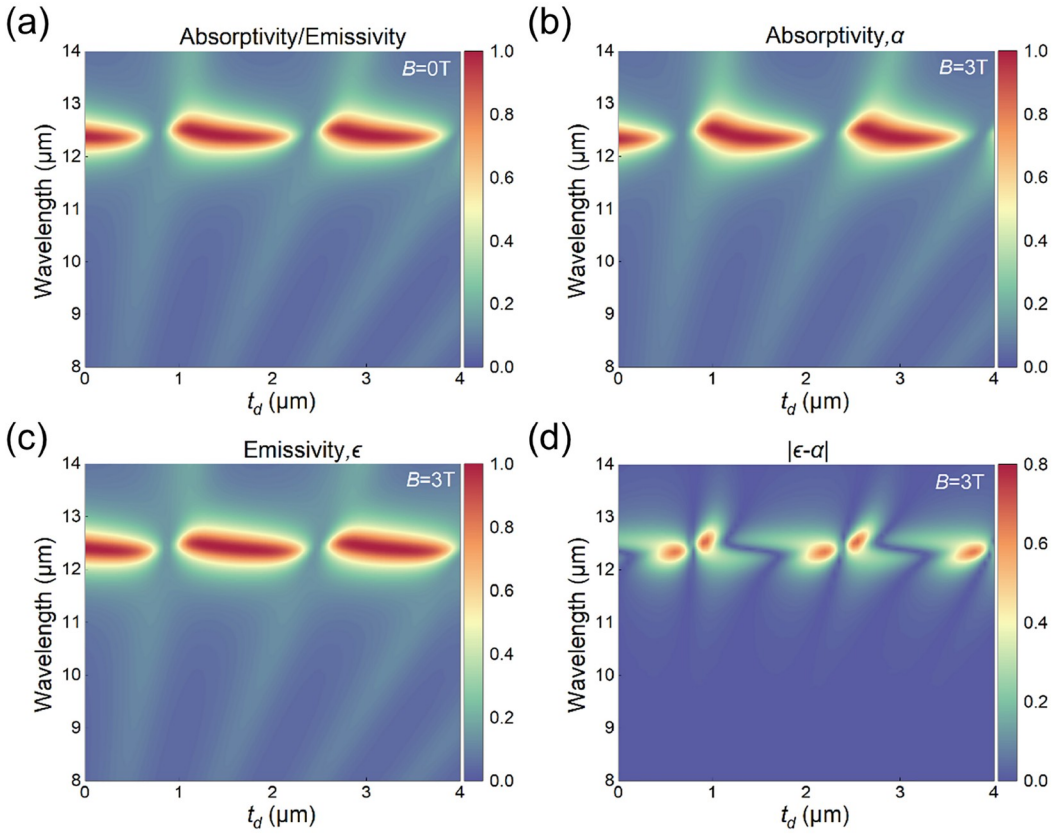

Figure 3 (Color online) Simulated spectra of the sandwich structure varying with the thickness of the DL t_d and wavelength when the incident angle is 70°. (a) Absorptivity/emissivity spectra with B = 0 T; (b) absorptivity spectra with B = 3 T; (c) emissivity spectra with B = 3 T; (d) difference between absorptivity and emissivity with B = 3 T.

absence of an external magnetic field. At this time, no nonreciprocity phenomenon occurs, and the absorption/emission intensity periodically increases and decreases with the increase in cavity thickness near the ENZ wavelength. When B = 3 T, the changes in the absorption and emission spectra with the DL thickness are shown in Figure 3(b) and (c), respectively. Compared with Figure 3(a), the overall absorption spectrum shifts to the left, whereas the overall emission spectrum shifts to the right because of the asymmetric dielectric tensor of MO material. To show the nonreciprocity more clearly, the difference between absorption and emission is calculated, as shown in Figure 3(d). The nonreciprocal thermal radiation also presents a periodic change with the increase in cavity thickness.

3.4 Influence of the refractive index of the DL

The influence of n_d on nonreciprocal thermal radiation is also explored. Figure 4(a)–(c) show the variations of the absorptivity, emissivity, and nonreciprocity of a sandwich structure with n_d. First, the absorption and emission spectra are significantly different under the asymmetric Berreman mode. Near the ENZ wavelength, the absorptivity decreases with the increase in the refractive index, whereas the emissivity remains high. Therefore, the degree of nonreciprocity gradually increases with the increase in the refractive index n_d, as shown in Figure 4(c). The investigation of the impact of the refractive index on nonreciprocal thermal radiation shows that in addition to choosing Ge as the DL, silicon (Si) can also play a role in strengthening nonreciprocal thermal radiation, providing more diverse material choices.

3.5 Influence of the DL on the gradient ENZ MOL

The theoretical work of placing a gradient ENZ MO thin film on a metal to achieve broadband nonreciprocal thermal radiation has been investigated [30]. However, when the ENZ wavelength is reduced to a certain degree, the degree of nonreciprocity will be considerably attenuated in the broadband nonreciprocal thermal radiation. Here, the effect of the Fabry–Perot cavity on nonreciprocal broadband thermal radiation is determined by replacing the top ENZ MOL with a gradient ENZ magneto-optical layer (GMOL) to form a GMOL–DL–ML sandwich structure, as shown in Figure 5(a).

The gradient ENZ layer consists of six layers of MO

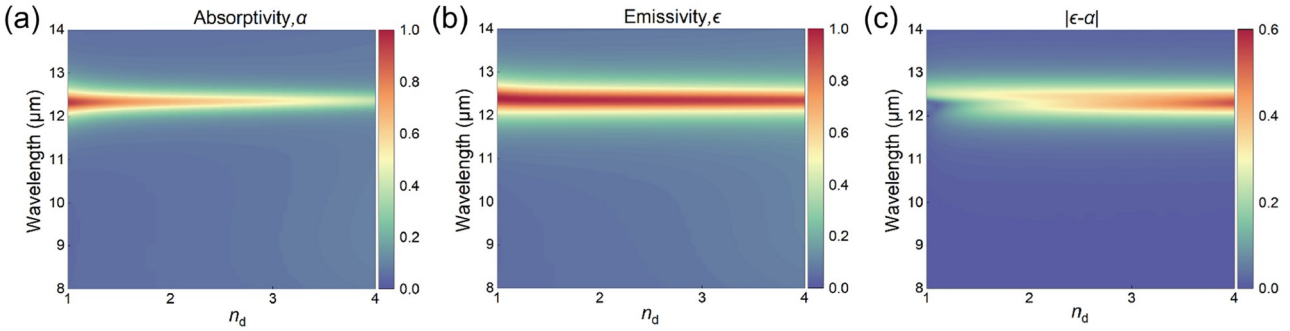

Figure 4 Simulated spectra of the sandwich structure varying with the refractive index of the DL n_d and wavelength when the incident angle is 70°. (a) Absorptivity spectra with B = 3 T; (b) emissivity spectra with B = 3 T; (c) difference between absorptivity and emissivity with B = 3 T.

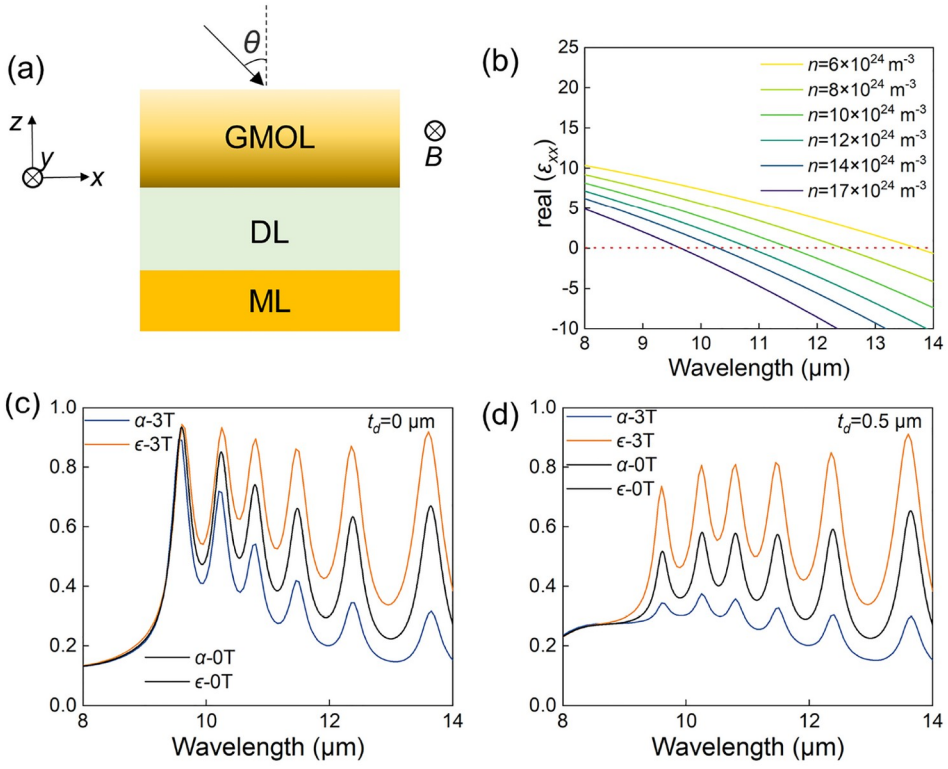

Figure 5 (a) Diagram of a broadband nonreciprocal thermal emitter shaped like a sandwich structure. (b) Permittivity varying with wavelength for different ENZ MO films. Absorptivity and emissivity spectra of the emitter with θ = 70°: without the DL (c) and with the DL (d).

material InSb with different doping concentrations. The doping concentration of gradient ENZ MO films gradually decreases along the z-axis, and the specific parameters of each ENZ film are shown in Table 1. To more clearly show the relationship between ENZ wavelength and doping concentration of MO materials, the changes of the real part of ε_{xx} with wavelength under different doping concentrations have been determined, as shown in Figure 5(b). Notably, the ENZ wavelength decreases with the increase in doping concentration.

To better show the effect of the Fabry–Perot cavity on broadband nonreciprocal thermal radiation, the absorption and emission spectra without and with the DL are calculated, as shown in Figure 5(c) and (d), respectively. Without the DL and with the applied magnetic field of 0, the absorption and emission spectra overlap and show broadband absorption and emission, which means that nonreciprocal thermal radiation is not achieved. When an external magnetic field is applied, absorption is suppressed, and emission is enhanced in the ENZ wavelength range, showing a broadband nonreciprocal effect [30]. However, as the ENZ wavelength decreases, nonreciprocity gradually decreases.

For the sandwich structure, as shown in Figure 5(d), the absorption and emission are weaker than that without the DL with B = 0 T, which indicates that the existence of the DL has a certain hindering effect on the excitation of the Berreman mode. However, when an external magnetic field is applied, the separation of the absorption and emission spectra is

greater in the ENZ wavelength range; that is, the broadband nonreciprocal thermal radiation effect is more significant, indicating that the Fabry–Perot cavity can strengthen the asymmetric Berreman mode. Here, to more intuitively show the influence of the Fabry–Perot cavity on broadband nonreciprocal thermal radiation, the parameter φ is defined to represent the degree of average wavelength nonreciprocity over a wide spectrum, which is specifically expressed as follows:

$$\varphi = \frac{|\epsilon_{\mathrm{ave}} - \alpha_{\mathrm{ave}}|}{\{\epsilon_{\mathrm{ave}}, \alpha_{\mathrm{ave}}\}_{\mathrm{max}}}, \tag{10}$$

where ϵ_{ave} and α_{ave} are the average emissivity and average absorptivity over a wide spectrum, respectively. In addition, $\{\epsilon_{\mathrm{ave}}, \alpha_{\mathrm{ave}}\}_{\mathrm{max}}$ is the maximum value of the average emissivity and average absorptivity. According to Eq. (10), when the band ranges from 9.5 to 14 μm, the values of φ without and with the DL are 0.455 and 0.558, respectively. Notably, the existence of the Fabry–Perot cavity can further enhance the effect of the broadband nonreciprocal thermal radiation.

Finally, the influence of the incident angle on the broadband nonreciprocal thermal radiation is discussed, as shown in Figure 6. First, without the DL, the changes of absorptivity and emissivity with the incident angle are calculated, as shown in Figure 6(a) and (b), respectively. Notably, in the ENZ wavelength range, the absorption intensity is weaker than the emission intensity, and the larger the wavelength is, the more obvious the nonreciprocity effect, which has been demonstrated in the literature [30]. In this work, based on the original, the GMOL–DL–ML sandwich structure has been considered, and the spectral effect is shown in Figure 6(d) and (e). In the ENZ wavelength range, the absorption intensity is further suppressed, and the emission intensity still maintains a strong broadband emission effect at the design

Table 1 Specific parameters of different ENZ MO films

n (10^{24} m^{-3})	μ_{n} (cm^2 V^{-1} s^{-1})	λ_{ENZ} (μm)	t_{MO} (μm)
6	7350	13.72	0.36
8	6400	12.445	0.31
10	5540	11.54	0.286
12	5070	10.85	0.26
14	4720	10.305	0.24
17	4330	9.65	0.215

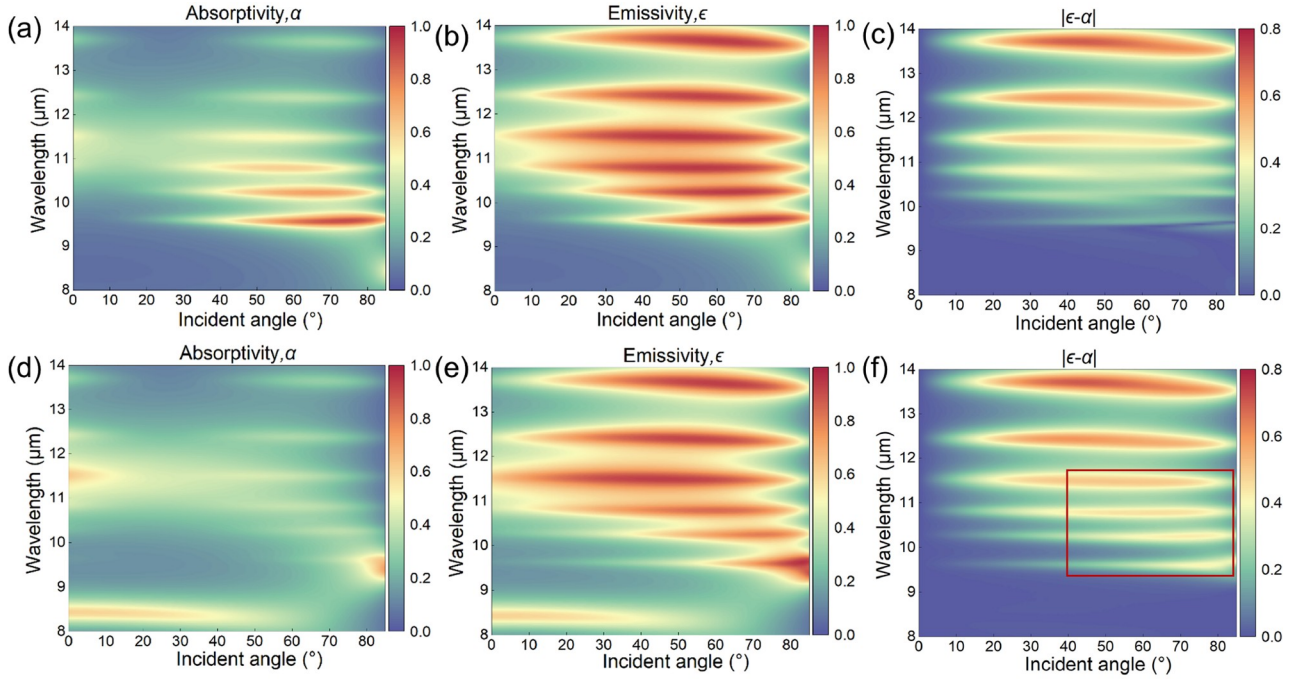

Figure 6 (Color online) Simulated spectra varying with the incident angle and wavelength of the broadband emitters with B = 3 T. Absorptivity spectra: without the DL (a) and with the DL (d). Emissivity spectra: without the DL (b) and with the DL (e). Difference between absorptivity and emissivity: without the DL (c) and with the DL (f).

angle (θ = 70°), which can achieve a stronger and more uniform nonreciprocal effect.

Here, to better compare the nonreciprocal effects of the two structures, the difference between absorption and emission is calculated, as shown in Figure 6(c) and (f). The sandwich structure with the DL has a more obvious nonreciprocal effect than the sandwich structure without the DL, and the smaller the ENZ wavelength is, the better the enhancement effect, which indicates the strengthening effect of the Fabry–Perot cavity on broadband nonreciprocal thermal radiation.

4 Conclusions

In this work, a sandwich structure consisting of the ENZ MOL, DL, and ML, which can achieve strong nonreciprocal effects in the long-wave infrared band, is proposed. The analysis of the internal mechanism shows that the strong nonreciprocal effect is mainly attributed to the strengthening effect of the existence of the Fabry–Perot cavity on the asymmetric Berreman mode. In addition, by replacing the top ENZ MOL with the GMOL, the change of single-band nonreciprocal thermal radiation to broadband nonreciprocal thermal radiation is realized. To better characterize the degree of broadband nonreciprocity, the parameter φ is proposed to characterize the degree of mean wavelength nonreciprocity in a wide band. The values of the parameter φ with and without the DL are 0.558 and 0.455, respectively, indicating that the existence of the DL can further improve the design effect of the existing broadband nonreciprocal thermal radiation. The proposed work promotes the development and application of broadband nonreciprocal energy devices.

This work was supported by the National Natural Science Foundation of China (Grant Nos. 52211540005 and 52076087), the Natural Science Foundation of Hubei Province (Grant No. 2023AFA072), the Open Project Program of Wuhan National Laboratory for Optoelectronics (Grant No. 2021WNLOKF004), Wuhan Knowledge Innovation Shuguang Program, and the Fundamental Research Funds for the Central Universities (Grant No. YCJJ20242102).

1 Kim L, Kim S, Jha P K, et al. Mid-infrared radiative emission from bright hot plasmons in graphene. Nat Mater, 2021, 20: 805–811
2 Shahsafi A, Roney P, Zhou Y, et al. Temperature-independent thermal radiation. Proc Natl Acad Sci USA, 2019, 116: 26402–26406
3 Zhang S X, Wang J C, Zhao Y M, et al. High-dielectric loss black silicon decorated with multi-nanostructure for wide-band mid-infrared absorption. Rare Met, 2023, 42: 2447–2456
4 Zhang B W, Fang D, Fang X, et al. InAs/InAsSb type-II superlattice with near room-temperature long-wave emission through interface engineering. Rare Met, 2021, 41: 982–991
5 Long M, Wang Y, Wang P, et al. Palladium diselenide long-wavelength infrared photodetector with high sensitivity and stability. ACS Nano, 2019, 13: acsnano.8b09476
6 Peng C Y, Wang B, Yuan L F, et al. Six- and five-coordinated Cr^{3+} in Ga_2GeO_5 invokes tunable broadband near-infrared emission toward night-vision applications. Rare Met, 2023, 42: 3787–3796
7 Nakazawa T, Kim D, Kim J, et al. Development of RuS_2 for near-infrared photodetector by atomic layer deposition and post-sulfurization. Rare Met, 2022, 41: 3086–3099
8 Zhu H, Li Q, Tao C, et al. Multispectral camouflage for infrared, visible, lasers and microwave with radiative cooling. Nat Commun, 2021, 12: 1805
9 Li W, Shi Y, Chen Z, et al. Photonic thermal management of coloured objects. Nat Commun, 2018, 9: 4240
10 Chen Q, Lu Y, Zhang J, et al. Flexible structural polyethylene films for dynamically tunable energy harvesting from the sun and outer space. Nano Energy, 2023, 114: 108610
11 Kim K, Song B, Fernández-Hurtado V, et al. Radiative heat transfer in the extreme near field. Nature, 2015, 528: 387–391
12 Li Y, Li W, Han T, et al. Transforming heat transfer with thermal metamaterials and devices. Nat Rev Mater, 2021, 6: 488–507
13 Zhang W B, Wang B X, Xu J M, et al. High-quality quasi-monochromatic near-field radiative heat transfer designed by adaptive hybrid Bayesian optimization. Sci China Tech Sci, 2022, 65: 2910–2920
14 Liang J, Hu M, Kan Q, et al. Infrared transition properties of vanadium dioxide thin films across semiconductor-metal transition. Rare Met, 2011, 30: 247–251
15 Xie T, Xu K D, Yang B L, et al. Effect of pore size and porosity distribution on radiation absorption and thermal performance of porous solar energy absorber. Sci China Tech Sci, 2019, 62: 2213–2225
16 Xu Z G, Hu Z F. Near-field radiative heat transfer enhancement by multilayers and gratings in the thermophotovoltaic system. Sci China Tech Sci, 2023, 66: 2968–2977
17 Zhu L, Fan S. Near-complete violation of detailed balance in thermal radiation. Phys Rev B, 2014, 90: 220301
18 Wang H, Qi D. Omnidirectional infrared nonreciprocal absorbers based on CdTe gratings. Int J Heat Mass Transfer, 2019, 135: 142–148
19 Zhao B, Shi Y, Wang J, et al. Near-complete violation of Kirchhoff's law of thermal radiation with a 0.3 T magnetic field. Opt Lett, 2019, 44: 4203–4206
20 Pajovic S, Tsurimaki Y, Qian X, et al. Intrinsic nonreciprocal reflection and violation of Kirchhoff's law of radiation in planar type-I magnetic Weyl semimetal surfaces. Phys Rev B, 2020, 102: 165417
21 Zhao B, Guo C, Garcia C A C, et al. Axion-field-enabled nonreciprocal thermal radiation in Weyl semimetals. Nano Lett, 2020, 20: 1923–1927
22 Chen Z, Yu S, Hu B, et al. Multi-band and wide-angle nonreciprocal thermal radiation. Int J Heat Mass Transfer, 2023, 209: 124149
23 Shi K, Sun Y, Hu R, et al. Ultra-broadband and wide-angle nonreciprocal thermal emitter based on Weyl semimetal metamaterials. Nanophotonics, 2024, 13: 737–747
24 Shi K, Xing Y, Sun Y, et al. Thermal vertical emitter of ultra-high directionality achieved through nonreciprocal magneto-optical lattice resonances. Adv Opt Mater, 2022, 10: 2201732
25 Wu J, Wu B, Shi K, et al. Strong nonreciprocal thermal radiation of transverse electric wave in Weyl semimetal. Int J Therm Sci, 2023, 187: 108172
26 Khandekar C, Messina R, Rodriguez A W. Near-field refrigeration and tunable heat exchange through four-wave mixing. AIP Adv, 2018, 8: 055029
27 Buddhiraju S, Li W, Fan S. Photonic refrigeration from time-modulated thermal emission. Phys Rev Lett, 2020, 124: 077402
28 Liu M Q, Zhao C Y. Near-infrared nonreciprocal thermal emitters induced by asymmetric embedded eigenstates. Int J Heat Mass Transfer, 2022, 186: 122435
29 Wu J, Wang Z, Wu B, et al. The giant enhancement of nonreciprocal radiation in Thue-morse aperiodic structures. Optics Laser Tech, 2022, 152: 108138
30 Zhang Z, Zhu L. Broadband nonreciprocal thermal emission. Phys Rev Appl, 2023, 19: 014013

31 Liu M, Xia S, Wan W, et al. Broadband mid-infrared non-reciprocal absorption using magnetized gradient epsilon-near-zero thin films. Nat Mater, 2023, 22: 1196–1202
32 Wu J, Li H, Fu C, et al. High quality factor nonreciprocal thermal radiation in a Weyl semimetal film via the strong coupling between tamm plasmon and defect mode. Int J Therm Sci, 2023, 184: 107902
33 Guo C, Asadchy V S, Zhao B, et al. Light control with Weyl semimetals. eLight, 2023, 3: 2
34 Litwin-Staszewska E, Szymańska W, Piotrzkowski R. The electron mobility and thermoelectric power in InSb at atmospheric and hydrostatic pressures. Physica Status Solidi (b), 1981, 106: 551–559
35 Law S, Liu R, Wasserman D. Doped semiconductors with band-edge plasma frequencies. J Vacuum Sci Tech B, 2014, 32: 052601
36 Ying Y, Ma B, Yu J, et al. Whole LWIR directional thermal emission based on ENZ thin films. Laser & Photonics Rev, 2022, 16: 2200018
37 Wu J, Qing Y M. Nonreciprocal thermal emitter for near perpendicular incident light with cascade grating involving weyl semimetal. Mater Today Phys, 2023, 32: 101025